Testing of the C1 Coil

September 15, 2006

NCSX-TEST-14-01-00

DRAFT

Prepared by: _____

Wayne Reiersen

Reviewed by: _____

Geoff Gettelfinger

Reviewed by: _____

Kevin Freudenberg

Reviewed by: _____

David Williamson

Reviewed by: _____

Art Brooks

Approved by: _____

Brad Nelson

Table of Contents

Table of Tables

Table of Figures

1 EXECUTIVE SUMMARY

The C1 modular coil was tested in the NCSX Coil Test Facility in June 2006. The goals of the testing were to verify that the coils behave as predicted, thus validating our analytical models, and to qualify a system for monitoring the structural behavior of the modular coils during experimental operations. All of the modular coils will be tested at room temperature as part of the manufacturing procedures. Room temperature tests include resistance measurements, ground insulation and electrical break voltage tests, and flow and leak tests of the coolant tubes. In addition, the project will implement AC tests to measure the coil inductance and capacitance.

The coil was cooled down to cryogenic temperature and tested at full current. The coil resistance, the observed temperature rise, and the cooldown rate were all in agreement with predicted values. Displacements across the width of the coil were measured with a displacement gage and were also in agreement with predicted values.

Conventional (resistive) strain gages were applied to the winding form and winding pack. These gages were used because of previous favorable experience on ATF. Bench tests were conducted prior to testing C1 that confirmed that these gages could be used in a cryogenic environment. However, the test data from these gages during testing of the C1 coil was not usable. Examination of the test data revealed that the substantial voltage ripple in the power supply and magneto-resistive effects in the strain gages precluded getting useful data. Using fiber optic strain gages that would be immune to these effects is being considered.

2 TEST SETUP

2.1 Instrumentation

2.1.1 Thermocouples

Eighteen Type E thermocouples were installed in the test setup. The data acquisition system provided six channels for thermocouple data. The locations for the thermocouples are listed in Table 5-1. Two thermocouples (TC2 and TC3) were embedded in deep holes in the winding form. One thermocouple was installed on the exterior of the winding pack (TC17). One thermocouple was installed on an inboard supply coolant tube (TC7) and another on an outboard return coolant tube (TC9). Thermocouples were typically insulated with bat insulation from the cryostat environment to avoid convective cooling of the thermocouple directly. The final channel monitored the temperature inside the cryostat near the midplane elevation (TC18).

2.1.2 Strain gages

Fifteen strain gages were installed. The strain gages were manufactured by Vishay (H06A-AC1-125-700). The data acquisition system provided fourteen operable channels for the strain gage data. The locations for the strain gages are listed in Table 5-2. Of the fourteen operable channels, ten channels monitored strain gages mounted on the winding form. Nine of these strain gages were mounted at the base of the tee. The tenth was mounted on the exterior surface of the winding form near where the leads penetrate the winding form. The active strain gages mounted on the winding form were paired with dummy strain gages mounted approximately 1 inch off the winding form on a stainless steel substrate connected to the casting with a stud. Strain gages were typically insulated with bat insulation to avoid introducing temperature differences between the active and dummy gages due to convective cooling. Some strain gages, e.g., SG15, had a copper sleeve around the stud for improved thermal contact. The intent of the dummy gages was to remove the thermal output so the apparent strain reflected the true mechanical strain. Photographs of strain gage installations (without thermal insulation) are provided in Figure 7-11 through Figure 7-16.

The remaining four strain gages were installed on the exterior of the winding pack. There was no substrate to mount dummy gages so the dummy gage was actually installed on the winding pack on the opposite side of the tee. This was intended to remove the thermal output from cooldown to cryogenic temperature. However, the apparent strain due to EM loading during a pulse would be the difference between these two active gages. Strain gages mounted on the winding pack are apparent in Figure 7-11.

The strain gages mounted at the base of the tee and on the winding pack were oriented either in the direction of the winding pack or normal (transverse) to the direction of the winding pack. Typically, two strain gages, one in the direction of the winding pack and one in the transverse direction were installed at each of the clamp locations selected as shown in Figure 7-13.

2.1.3 Deflection monitor

A deflection monitor was mounted on the flanges to measure the linear deflection across the bore of the coil during a pulse. The gage and digital readout were located outside the cryostat. The readings on the digital readout were recorded with a videocamera.

3 TEST RESULTS

3.1 Cooldown

Cooldown of the C1 coil began on June 11 and continued until shots began to be taken on June 15. Cooldown was initiated by introducing product from the LN2 supply line. The line is used intermittently so initially, the product was warm gas. A maximum temperature difference of 50K was administratively enforced during cooldown. As the line cooled, so did the gas being supplied until eventually it became 2-phase product and then liquid. The liquid was caught in a tank in the center of the cryostat. The tank measured 12” on each side. The liquid column was approximately 28” tall.

During the first 40 hours, the cooldown followed an exponential curve that featured a decay time of 18 hours with an asymptote of approximately 120K. The cooldown versus time for one of the thermocouples embedded in the winding form is shown in Figure 3-1.

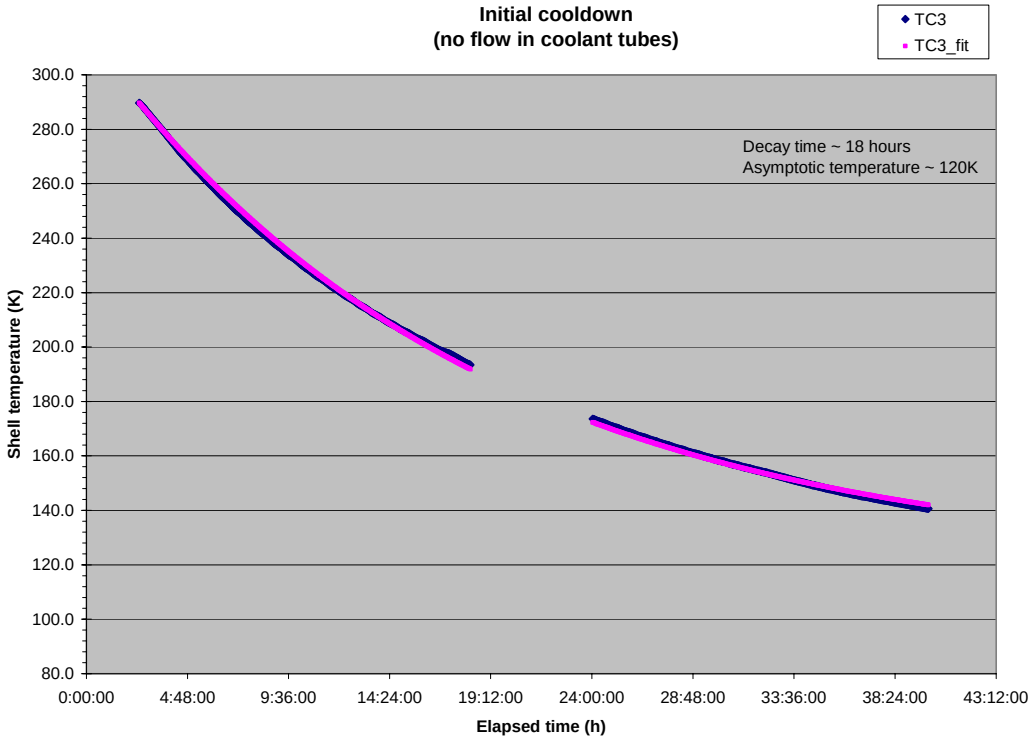

Figure 3-1 Winding form cooldown versus time

The SRD requirement is for the modular coils to be cooled down to operating temperature (nominally 80K) within 96 hours. Cooling from 293K to 90K assuming an 85K interior temperature would require a decay time of 25 hours (if an exponential model applied). The cooldown of C1 was based on cooling the interior and exterior of the shell. In the stellarator, the space between the modular coil and vacuum vessel (the interior of the shell) will be filled with insulation. Therefore, the surface area exposed to GN2 will be reduced by more than half. The decay time should be inversely proportional to the exposed surface area and the convective heat transfer coefficient. The decrease in surface area will have to be compensated by an increase in the convective heat transfer coefficient. This may require a change from natural (free) convection to forced convection.

The asymptotic (bath) temperature of the cryostat was well above the desired 80K. This too needs to be addressed in the cryostat cooling system design. In equilibrium, the cryostat system can be modeled as shown in Figure 3-2.

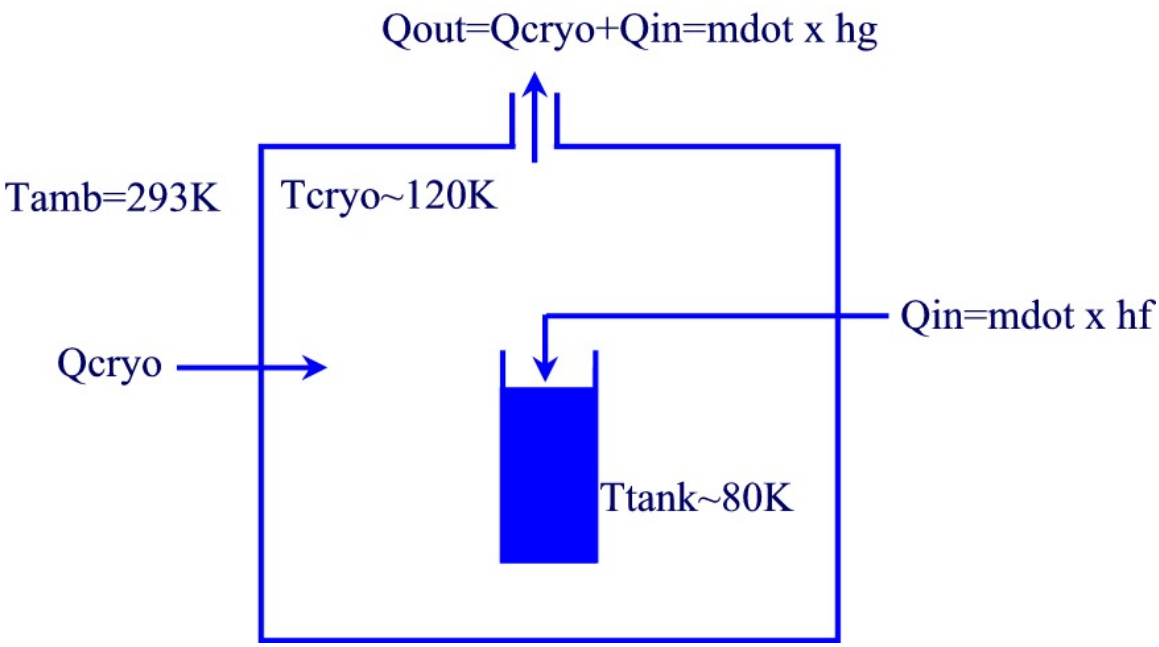

Figure 3-2 Cryostat heat balance

Assuming a surface area of 32 m2 for the cryostat and a 6-inch wall of panels with an insulating value of R6 per inch, the heat leak into the cryostat would be approximately 860 W. If the temperature of the exhaust gas is 120K (the asymptotic temperature calculated for initial cooldown), then a mass flow of 0.0036 kg/s is required. Two thirds of the heat is removed by evaporating LN2 with the balance removed by the temperature rise in the exhaust gas. In the stellarator, we want to minimize any temperature rise in the exhaust gas in order to keep the temperature as close to 80K as possible.

When the temperature inside the cryostat approached 130K, 2-phase product was introduced into the coolant channels. Ultimately, single phase LN2 was circulated through the winding pack which brought the chamber down in temperature to 100K (TC18 in Figure 3-3) in approximately ten (10) hours. This temperature was well above the 80K temperature envisioned for the coil environment. Thermocouples embedded in the winding form near the winding pack read as low as 92K (TC3) and 94K (TC2). The inlet temperature read as low as 83K (TC7) with an outlet temperature of 87K (TC9). Note that the beneficial effect of cooling the chamber brought about be cooling the winding pack with LN2 will not be manifest (at least not directly) in the stellarator because the winding pack will be thermally insulated. Note also that there were no measurements of the winding form temperature apart from the two thermocouples embedded deep in the winding form close to the winding pack. Additional thermocouples should be provided on the winding forms in the stellarator so temperature differences can be monitored.

The temperature of the winding form in the wings was not monitored. In the stellarator, this is an area of concern. The plasma-side surface of the wings is thermally insulated. The outside surface faces, but is not in good thermal contact with the plasma-side surface of the winding form into which it nests. It may be beneficial, perhaps necessary, to circulate gaseous nitrogen through the coolant tubes in order to cool the wings and also expedite initial cooldown.

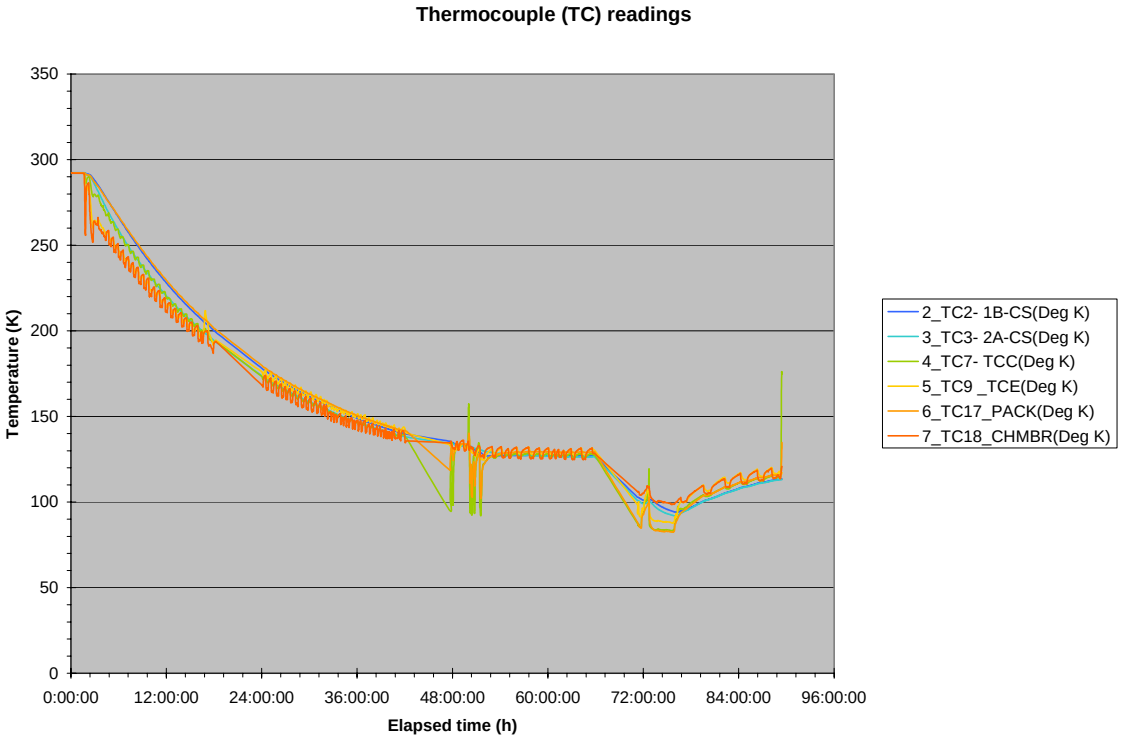

Figure 3-3 Thermocouple readings during initial cooldown

3.2 Coil testing

A series of shots were taken with the coil cold on June 15 and June 16. Coil currents were increased from 5kA to 36.5kA. Coil currents were then decreased down to 15kA. The prescribed waveform was the same for all of the test shots. There was a 1s linear rise to full current, a 0.2s flattop, and a 1s linear ramp down to zero current. Intermediate 2kA shots were taken at approximately 10 minute intervals to measure the coil resistance and infer the average winding temperature. Test shots (above 2kA) were not initiated unless the coil resistance measured in the 2kA shots was at or below 1.8 milli-ohms which corresponds to an average winding temperature of approximately 98K. The coil was then allowed to warm back to room temperature during which time additional 15kA shots were taken. The sequence is shown in Table 3-1. 2kA shots and shots in which there were trips are not shown. All test data is available from the following URL:

http://ncsx.pppl.gov/NCSX_Engineering/R&D_Results/PPPL/C1%20Testing/Index_C1%20testing.htm

The purpose of the test shots is to validate our modeling of coil performance. If we successfully predict the performance of the C1 coil in the test shots, then we have increased confidence in the predicted performance during stellarator operation. There are several aspects of coil performance to be modeled, including [1] cooldown between shots; [2] thermal stresses from initial cooldown; and [3] incremental stresses and displacement due to EM loads during a shot.

Table 3-1 Summary of test shots

Shot number	Date and time	Max current (kA)	Pre-shot outlet (TC9) temperature (K)
121400	6/15 2:54:31pm	5	87.2
121405	6/15 3:33:43pm	15	87.6
121408	6/15 3:52:39pm	25	87.6
121419	6/16 9:54:18am	35	92.1
121439	6/16 12:06:43pm	36.5	89.6
121453	6/16 1:27:56pm	36.5	88.9
121461	6/16 2:31:55pm	36.5	88.8
121468	6/16 3:33:33pm	25	88.6
121471	6/16 3:59:03pm	15	88.6
121537	6/23 9:29:30am	15	256.0
121540	6/23 10:14:37am	15	258.2

3.2.1 Cooldown between shots

There are two diagnostics from which we can monitor cooldown between shots. The first diagnostic is the thermocouple data. The was a thermocouple mounted on the outside of the winding pack near hole 85 (TC17). The second diagnostic is the temperature inferred from the 2kA shots run between test shots.

Consider cooldown following Shot 121461 which was a full current (36.5kA) shot. A plot is shown in Figure 3-4. The thermocouple mounted on the surface of the winding pack (TC17) starts off with a temperature reading of 83.2K which is approximately equal to the inlet temperature reading 83.8K (TC7). During a shot, the temperature of the winding pack is estimated to increase by approximately 28K within the 2.2s shot duration. The temperature of the chill plate under TC17 rises over the next 4 minutes by 5.3K. Thereafter, the temperature of the chill plates drops with a decay time of approximately 13 minutes. After 15 minutes, TC17 still reads 85.7K which is 2.5K higher than the initial temperature. In order to accommodate the soak time to establish the temperature gradients needed to conduct the heat to the coolant and the subsequent thermal decay time, it appears necessary to accept a pre-shot winding pack temperature which is significantly higher than the coolant temperature.

There are two phenomena that are occurring – temperature redistribution and cooling. The temperature on the surface of the winding pack can be approximated with a simple model per Equation 3-1.

Equation 3-1

$$T = T_a + (T_0 - T_a + \Delta T(1 - e^{-\alpha t}))e^{-\beta t}.$$

T_a is the asymptotic temperature to which the winding pack surface would decay and should approximate the local coolant temperature. T_0 is the initial temperature. ΔT is the increase in the surface temperature in the absence of cooling following a shot. α is the characteristic temperature redistribution rate. β is the characteristic heat removal rate. With an assumed coolant temperature of 83K (slightly less than the initial temperature of 83.2K), the "best fit" parameters are a ΔT of 9K, a characteristic temperature redistribution time ($1/\alpha$) of 2 minutes, and a characteristic cooling time ($1/\beta$) of 13 minutes. Although the adiabatic temperature rise in the copper conductor is calculated to be 28K, the winding form in the vicinity of the

winding pack acts as a heat sink as evidenced by the rise in temperatures in winding form thermocouples (TC2 and TC3). The assumed coolant temperature of 83K is reasonable because more than one hour transpired since the previous full current pulse. The agreement between the cooldown data following Shot 121461 and the simple model with these parameters is good as shown in Figure 3-5.

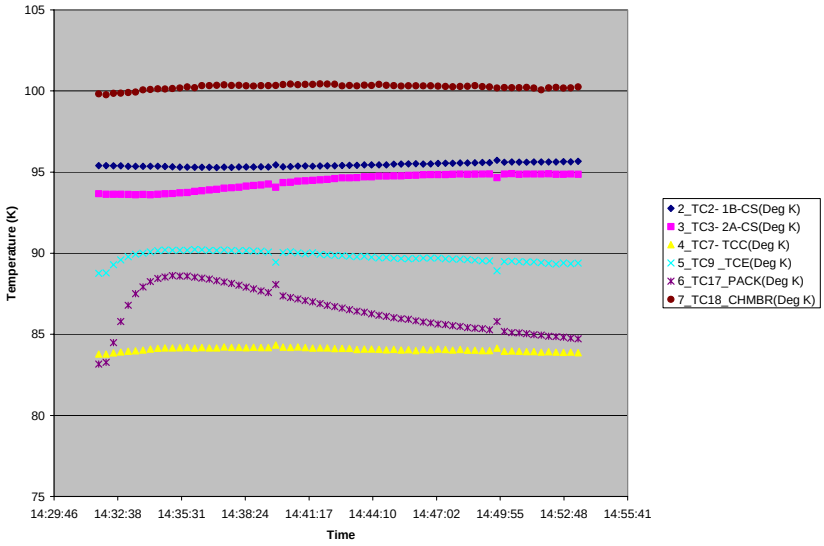

Figure 3-4 Cooldown following Shot 121461

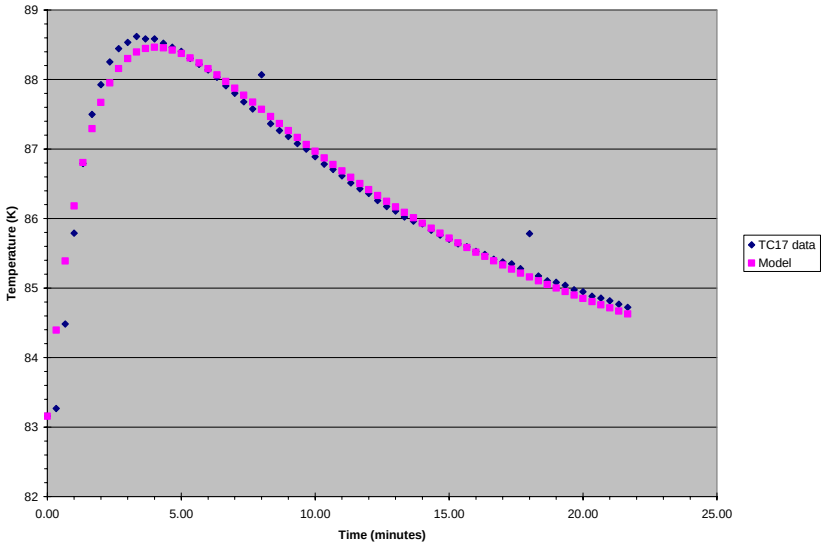

Figure 3-5 Winding surface temperature following Shot 121461

An ANSYS model of the winding pack was generated to model cooldown between pulses. The ANSYS model did not include the epoxy shell (of unknown thickness) outside the chill plates to which the thermocouple was attached. However, it is instructive to compare the thermal decay rate measured at thermocouple and predicted for the chill plates in the vicinity of the thermocouple. The cooldown between pulses of the chill plates is shown in Figure 3-6 for four points in time.

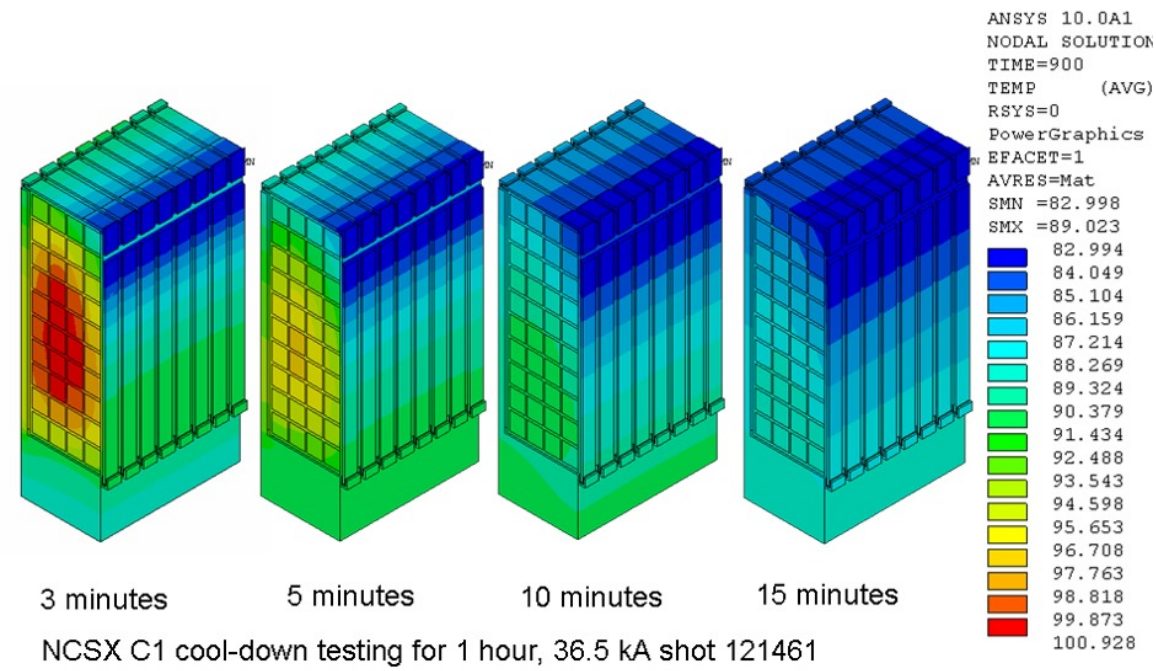

Figure 3-6 ANSYS modeling of cooldown following Shot 121461

Thermal decay rates along the height of the chill plate were calculated and matched well with the thermal decay rate observed for the thermocouple (TC17) mounted on the epoxy just outside the chill plate, closer to the coolant tubes than the base of the tee[1]. A comparison of the measured and calculated thermal decay rates (β in Equation 3-1) are shown in Figure 3-7.

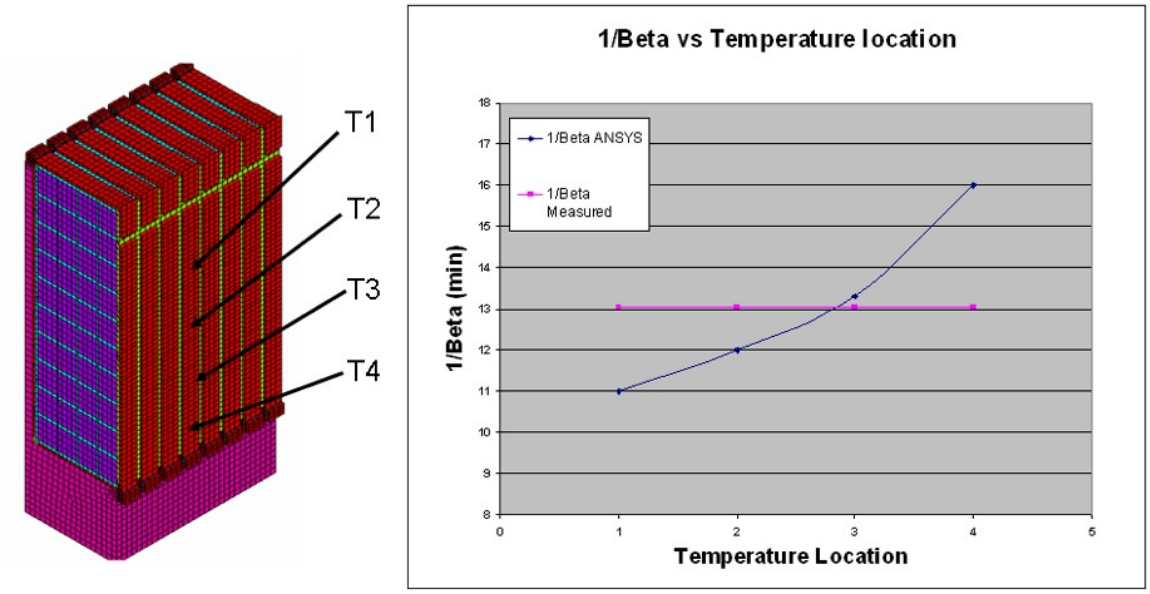

Figure 3-7 Comparison of measured and calculated thermal decay rates

[1] G. Gettelfinger, private communication

The second diagnostic is the average winding temperature inferred from the 2kA shots between test shots. The data is shown in Figure 3-8. Clearly, there is significant noise in the measurement and variation during a shot due to current redistribution among the four parallel conductors (even at constant net current). Shot 121462 was run at 2:40pm (8 minutes after Shot 121461) and registered a resistance in the range of 1.8-2.3 milli-ohms (2.05 milli-ohm median). Shot 121463 was run at 2:50pm (18 minutes after Shot 121461) and registered a resistance in the range of 1.5-2.0 milli-ohms (1.75 milli-ohm median). The median temperatures during Shots 121462 and 121463 are calculated to correspond to temperatures of 103.7K and 96.5K respectively.

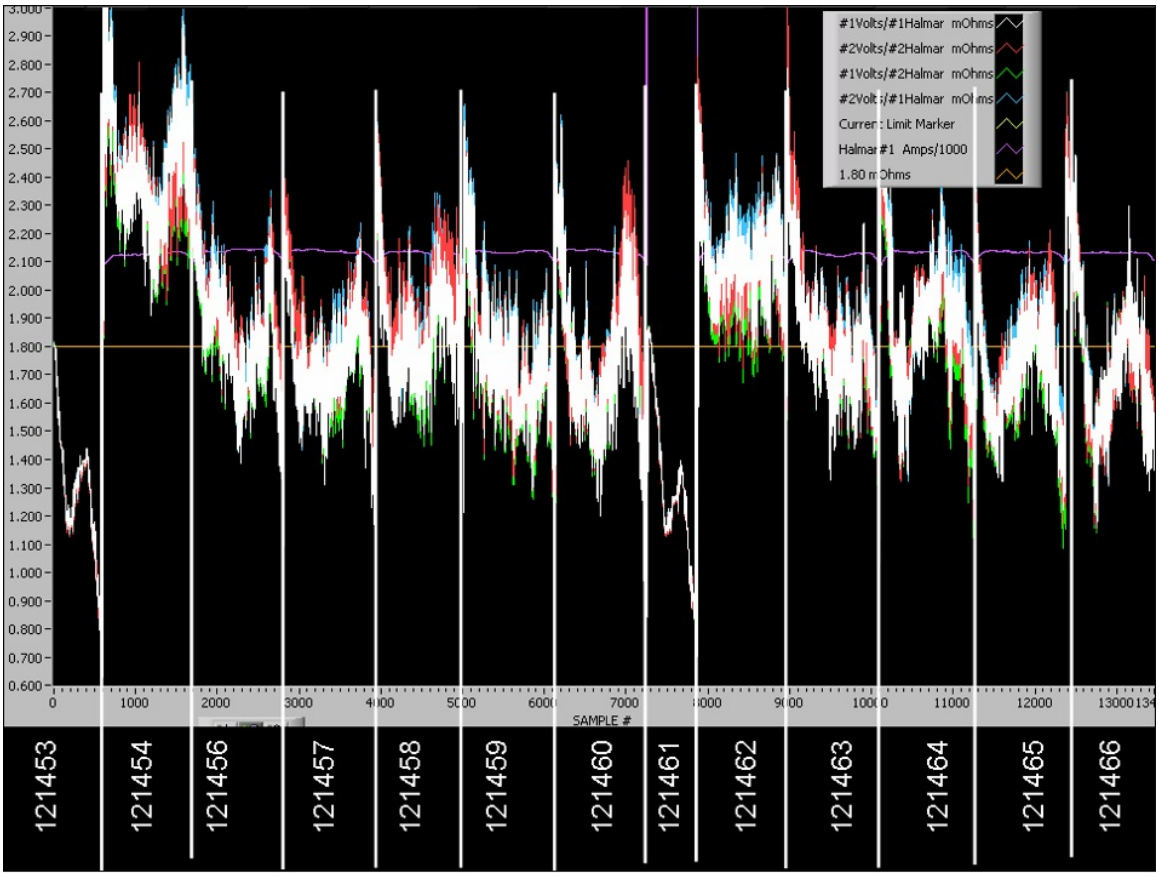

Figure 3-8 Winding resistance measurements

The coil resistance was measured manually (outside the cryostat) at 12:30pm prior to any shots. This measurement has none of the ripple associated with the 2kA shots. The resistance was measured to be 1.7 milli-ohms which corresponds to an average winding temperature of 89K. The outlet temperature of the coolant was also measured to be 89K at this time. If we assume that the asymptotic temperature of the winding pack (T_a) is 89K and the decay time is 13 minutes (as calculated for the winding pack surface), then the temperature rise during Shot 121461 (ΔT) is estimated to be 28K assuming the simple exponential model in Equation 3-2. The 28K temperature rise is consistent with adiabatic temperature rise predictions. The definitions in Equation 3-2 are the same as in Equation 3-1 except that the temperature rise is assumed to be instantaneous.

Equation 3-2

$$T = T_a + (T_0 - T_a + \Delta T)e^{-\beta t}$$

15 minutes after Shot 121461, the winding pack temperature is estimated to be 98K, well above the assumed pre-shot temperature of 89K. In order to cool down in 15 minutes without further thermal ratcheting, the starting temperature would need to be 95K with a coolant temperature of 80K per this simple model.

The ANSYS code was run to determine what temperature the winding pack would ratchet up to assuming an 80K coolant temperature and a 15 minute pulse repetition rate. The results are shown in Figure 3-9. The average conductor temperature is predicted to ratchet up to 92K after approximately six shots. No issues are apparent with starting a shot at this higher operating temperature.

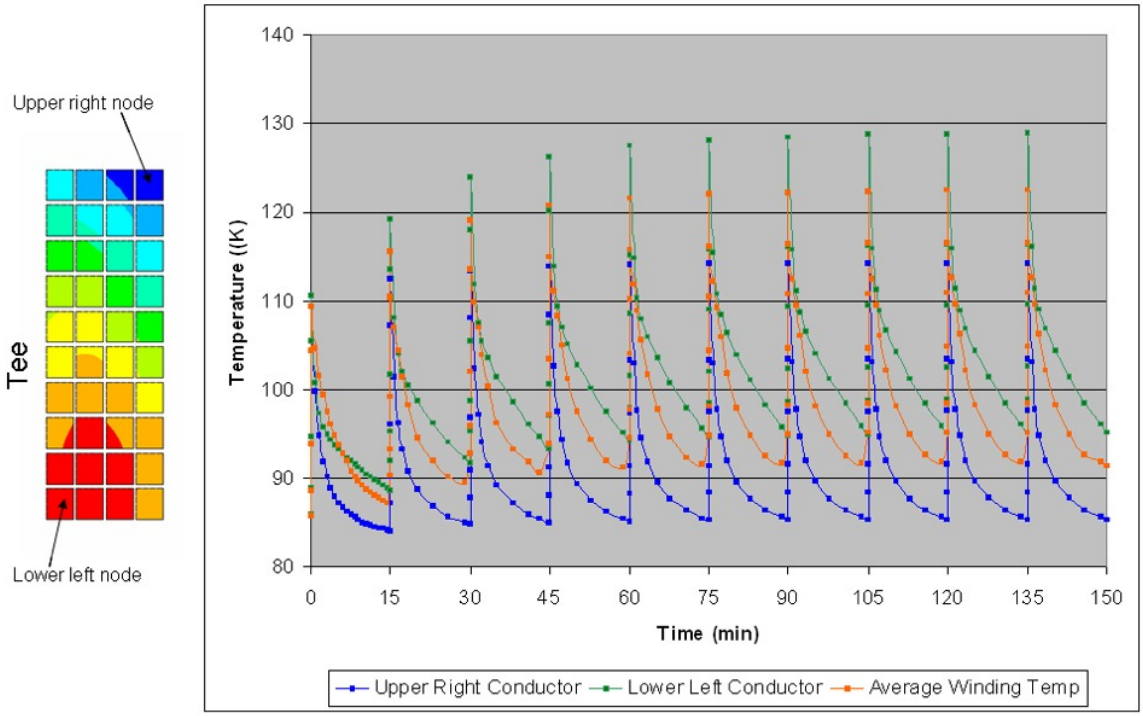

Figure 3-9 Evolution of conductor temperature during continual pulsing

3.2.2 Strain gage measurements

Strain gages were installed to measure strains, especially during a pulse when the peak strains which are due to EM loads are present. Comparing thermal strains to predictions is difficult because of the lack of thermocouple measurements in the vicinity of the strain gages. K. Freudenberg carefully reviewed the strain gage data. The results are provided in Section 6. The main conclusion was that the strain gage measurements are suspect and not usable. Supporting observations include the following:

- Room temperature data is very scattered when an applied voltage is present whereas the cryogenic data is highly linear.
- The room temperature data becomes smooth when the power supply trips, i.e. when there is no applied voltage but still substantial current. Even the cryogenic data is smoother after the trips.

- The programmed current waveforms are linear. On first principles, the strains due to EM loads should be quadratic with current. Instead, the strains appear linear with current, especially at cryogenic temperatures.
- Strain readings in orthogonal directions at the same approximate location give roughly the same strain due to EM loads. Data does not match ANSYS in direction or magnitude except at gage 15 which is in the lowest field region.

Examination of the voltage and current traces shows that the voltage ripple is extreme. For a nominal 100VDC, the observed voltage ripple was +/-200V. This might explain why the scatter in the room temperature data went away following a power supply trip. Constantan is used in the strain gages and is known to exhibit magneto-resistive properties, especially at cryogenic temperatures. This might explain why the magnitude and temporal profile of the strain measurements were so different from first principle expectations and ANSYS predictions. Recall that the measured displacement was consistent with ANSYS predictions. The implication is that the project needs to qualify a system for monitoring strain which is immune from power supply ripple and magnetic field effects.

4 CONCLUSIONS

- The coil resistance, the observed temperature rise, and the cooldown rate were all in agreement with predicted values.
- Displacements across the width of the coil were measured with a displacement gage and were also in agreement with predicted values.
- Test data from the conventional strain gages used for the C1 tests did not provide usable data. Strain gages which are immune to voltage ripple and magnetic field effects should be further investigated for project use.
- Careful attention should be given to the design of the cryostat cooling system to ensure that the coil cooldown requirement of 96 hours can be met.

5 REFERENCE TABLES AND FIGURES

Table 5-1 Thermocouple descriptions

Channel # Assignment	Thermocouple ID	Shell Hole number	Side	Location	Comments
Ch 1-bad	TC1_1A_CS	74		casting	
2	TC2_1B_CS	74		casting	
3	TC3_2A_CS	18		casting	
	TC4_2B_CS	18		casting	
	TC5_TCA				Supply Pipe
	TC6_TCB				Supply Outboard Pack
4	TC7_TCC				Supply Inboard Pack
	TC8_TCD				Return Outboard Pack
5	TC9_TCE				Return Outboard Pack
	TC10_TCF				Return Outboard Pack
	TC11_TCG				Return Outboard Pack
	TC12_TCH				Return Inboard Pack
	TC13_TCI				Return Inboard Pack
	TC14_TCJ				Return Inboard Pack
	TC15_TCK				Return Inboard Pack
	TC16_TCL				Return Lead Sides
6	TC17_PACK	85			Winding Pack
7	TC18_CHMBR				Chamber Temp
	TC19				
	TC20				

Table 5-2 Strain gage descriptions

S-Gage chan #	Strain Gage ID	Shell Hole number	Side	Location	Measuring Direction
1	SG1_7A_WP_W	7	A	winding pack	Winding direction
2	SG2_7A_CS_W	7	A	casting	Winding direction
3	SG3_7A_WP_X	7	A	winding pack	Transverse direction
CH 4 bad	SG4_14A_CS_W	14	A	casting	Winding direction
5	SG5_33A_CS_X	33	A	casting	Transverse direction
6	SG6_68B_WP_W	68	B	winding pack	Winding direction
7	SG7_68B_CS_W	68	B	casting	Winding direction
8	SG8_68B_WP_X	68	B	winding pack	Transverse direction
9	SG9_68B_CS_X	68	B	casting	Transverse direction
10	SG10_50B_CS_W	50	B	casting	Winding direction
11	SG11_50B_CS_X	50	B	casting	Transverse direction
12	SG12_50B_WP_W	50	B	winding pack	Winding direction
13	SG13_42A_CS_W	42	A	casting	Winding direction
14	SG14_68A_CS_W	68	A	casting	Winding direction
15	SG15_NLA_CS_P	Near Leads	Near A	Casting	Perpendicular to lead holes
16	SG16_7A_WP_W	*7*	*Redunanat for gage # 1*		
17	SG17_7A_CS_W	*7*	*Redunanat for gage # 2*		
18	SG18_68B_WP_W	*68*	*Redunanat for gage # 6*		
12	SG19_68B_CS_W	*68*	*Redunanat for gage # 7*		
20	SG20_42A_CS_W	*42*	*Redunanat for gage # 13*		

Strain gages in gray-scale rows not installed

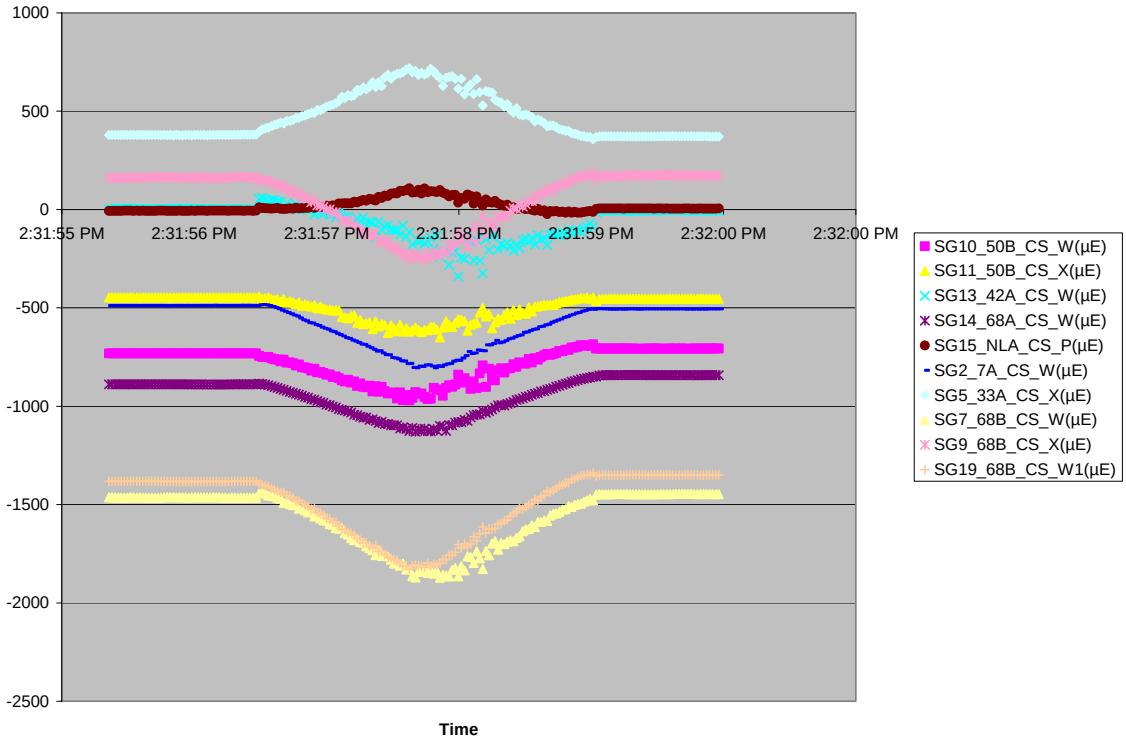

Figure 5-1 Strain gage data for Shot 121461 for strain gages mounted on the winding form

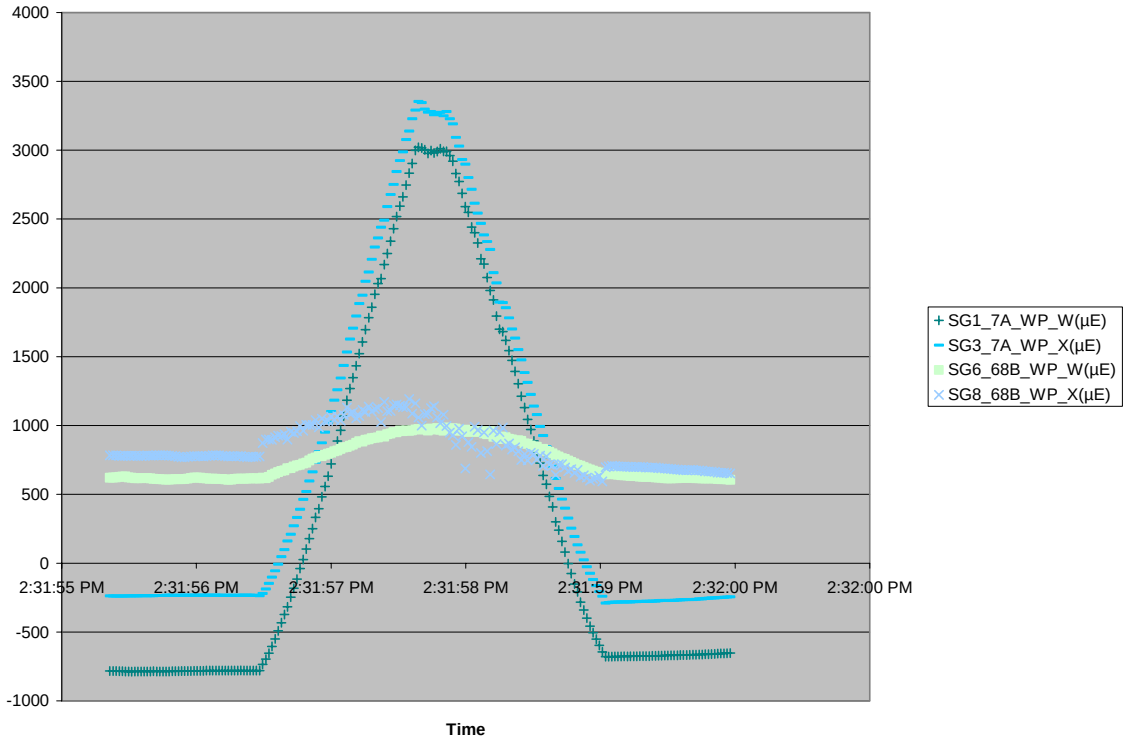

Figure 5-2 Strain gage data for Shot 1212461 for strain gages mounted on the winding pack

TEMPERATURE COEFFICIENT OF RESISTANCE FOR BONDABLE RESISTORS

NICKEL - Pure nickel has the highest resistance-versus-temperature sensitivity of the three most commonly used materials and is normally selected for span-versus-temperature compensation of transducers. The temperature coefficient of resistance is +0.33% per deg Fahrenheit (+0.59% deg Celsius) over a temperature range of +50 to +150 deg Fahrenheit (+10 to +65 deg Celsius).

BALCO - With a lower temperature coefficient of resistance (TCR) and a higher resistivity than nickel, Balco yields higher resistance values more easily. The TCR for Balco is +0.24% per deg Fahrenheit (+0.43% per deg Celsius) over the temperature range of +50 to +150 deg Fahrenheit (+10 to +65 deg Celsius).

COPPER - Pure copper has the lowest and most linear TCR, as well as the lowest resistivity of the three materials, making it ideal for smaller scale temperature compensations in transducers. The TCR for pure copper is +0.20% per deg Fahrenheit (+0.36% per deg Celsius).

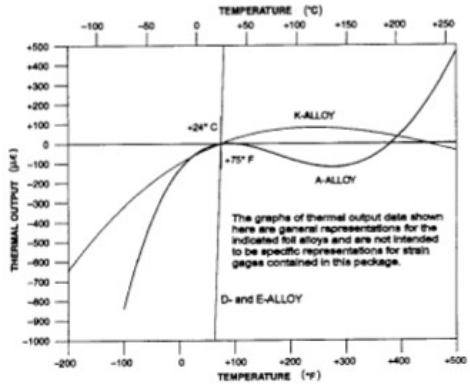

CALCULATION OF THERMAL OUTPUT FOR STRAIN GAGES

The thermal output of the gages contained in this package can be calculated from the following polynomial expression

$$a0 + a1*T + a2*T^2 + a3*T^3 + a4*T^4$$

where aN are the coefficients and T^N is temperature to the Nth power.

The coefficients for both Celsius and Fahrenheit temperature scales are provided on the data label affixed to this package for strain gages.

A-Alloy, D-Alloy, and E-Alloy will generally use all five coefficients (a0 to a4) but K-Alloy will generally use only the first four coefficients (a0 to a3) with the fifth (a4) being zero.

VISHAY MICRO-MEASUREMENTS & SR-4

Magnetic Field

STRAIN GAGES

FOR COMPLETE TECHNICAL DATA, VISIT WWW.VISHAY.COM/REF/STRAINGAGES

GRID RESISTANCE IN OHMS	T.C. OF GAGE FACTOR, %/100°C
700.0±0.5%	(+1.3±0.2)

GRID	GAGE FACTOR AT 24°C	TRANSVERSE SENSITIVITY
1	2.105±0.5%	(+0.6 ±0.2)%
2		
3		
NOM		

THERMAL OUTPUT COEFFICIENTS FOR 1018 STEEL

ORDER	FAHRENHEIT	CELCIUS
0	-1.19E+2	-4.11E+1
1	+3.22E+0	+3.12E+0
2	-2.62E-2	-6.61E-2
3	+6.31E-5	+3.40E-4
4	-3.75E-8	-3.94E-7

FOIL LOT NUMBER A44AD25 — BATCH NUMBER F374099

ITEM CODE	QUANTITY	CODE
7856	5	151321

MADE IN UNITED STATES

H06A-AC1-125-700

Technical notes from Vishay on strain gage technology can be found at the following URL:

http://www.vishay.com/brands/measurements_group/guide/indexes/tn_index.htm

Figure 5-3 Calculation of thermal output for strain gages

6 STRAIN GAGE EXPLORATIONS

(courtesy of K. Freudenberg)

15 Kamp Cold Test (121405)

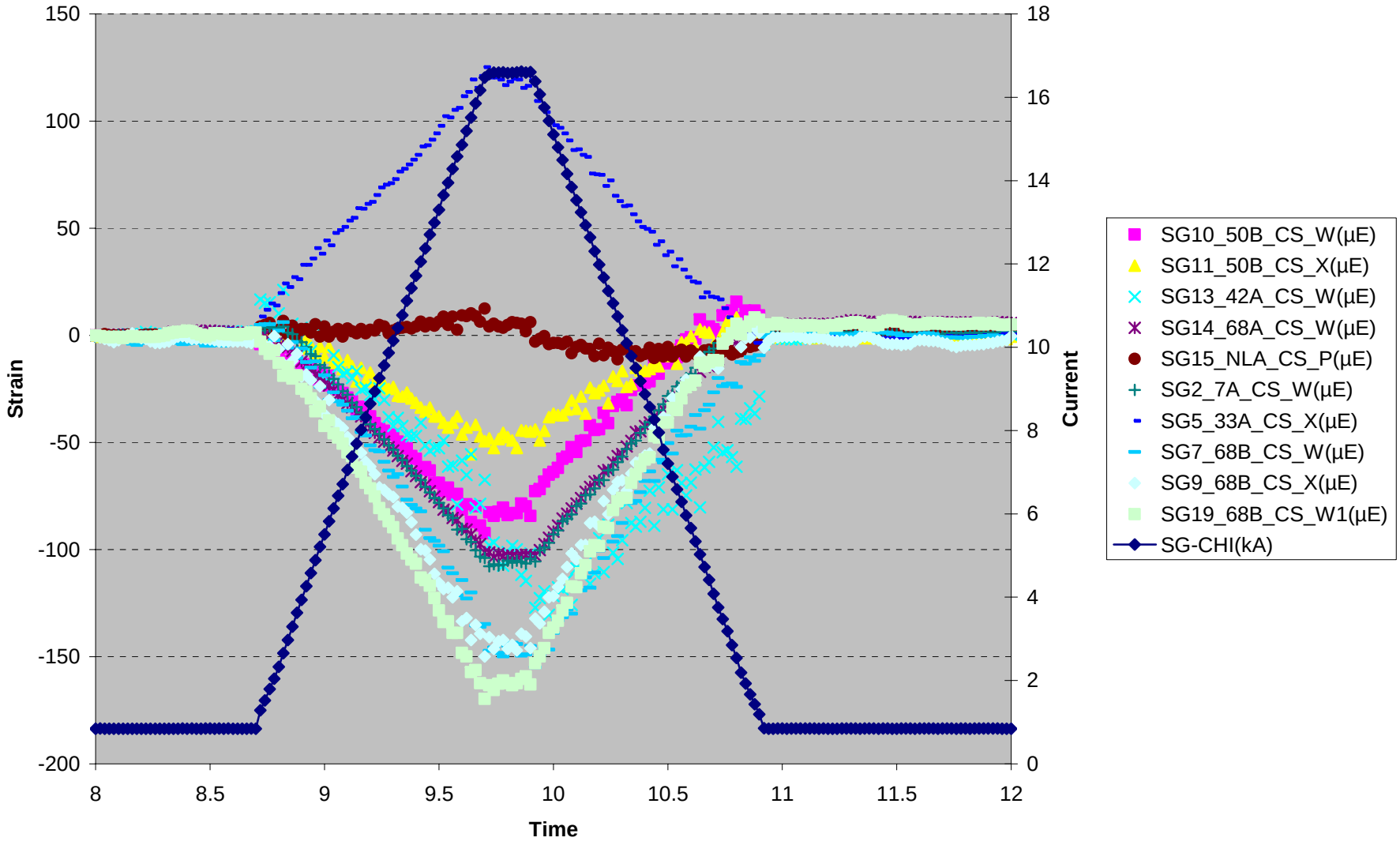

15 Kamp (warm test 121540)

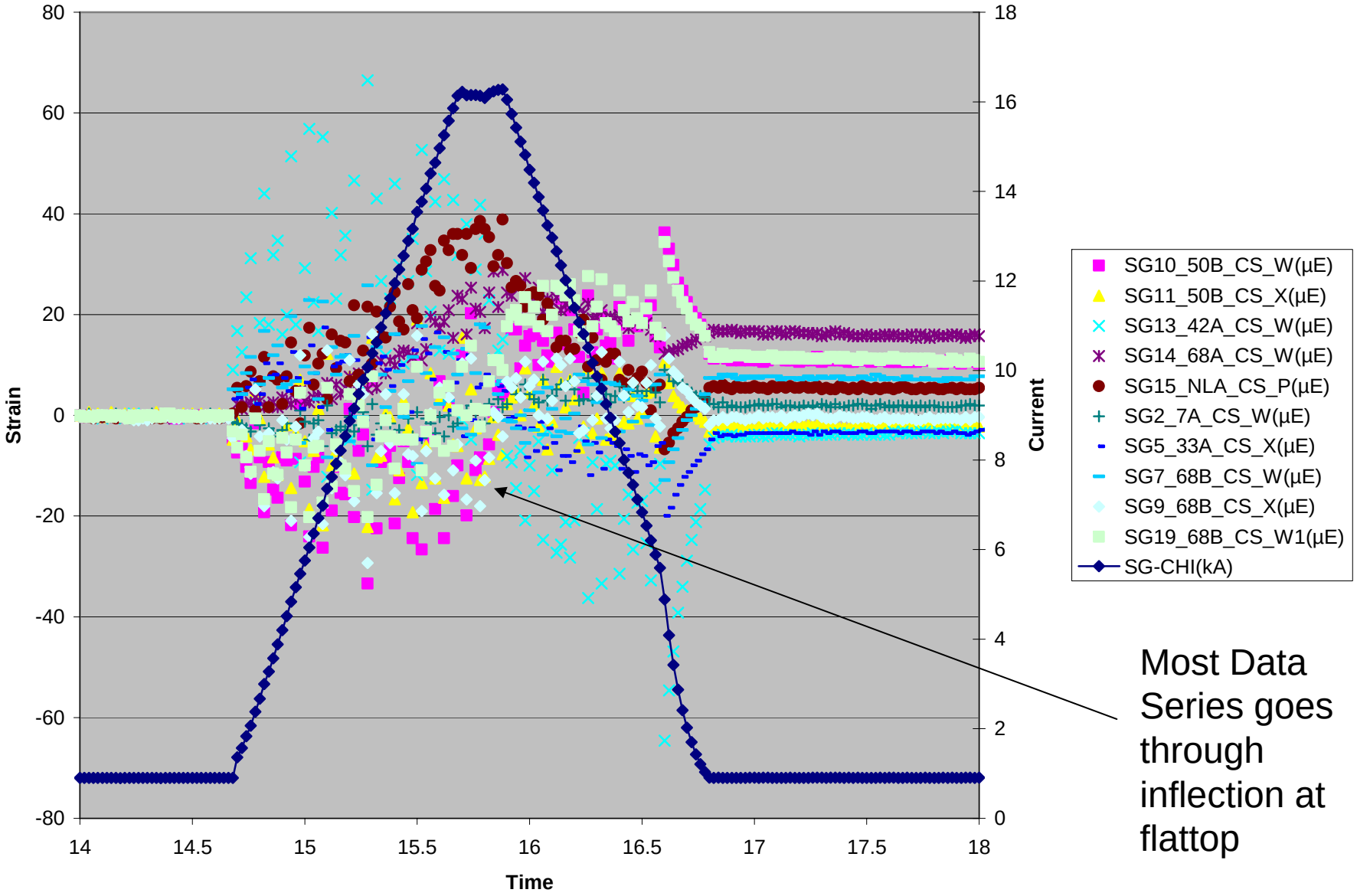

Most Data Series goes through inflection at flattop

15 kamp (warm) Case after trip ?

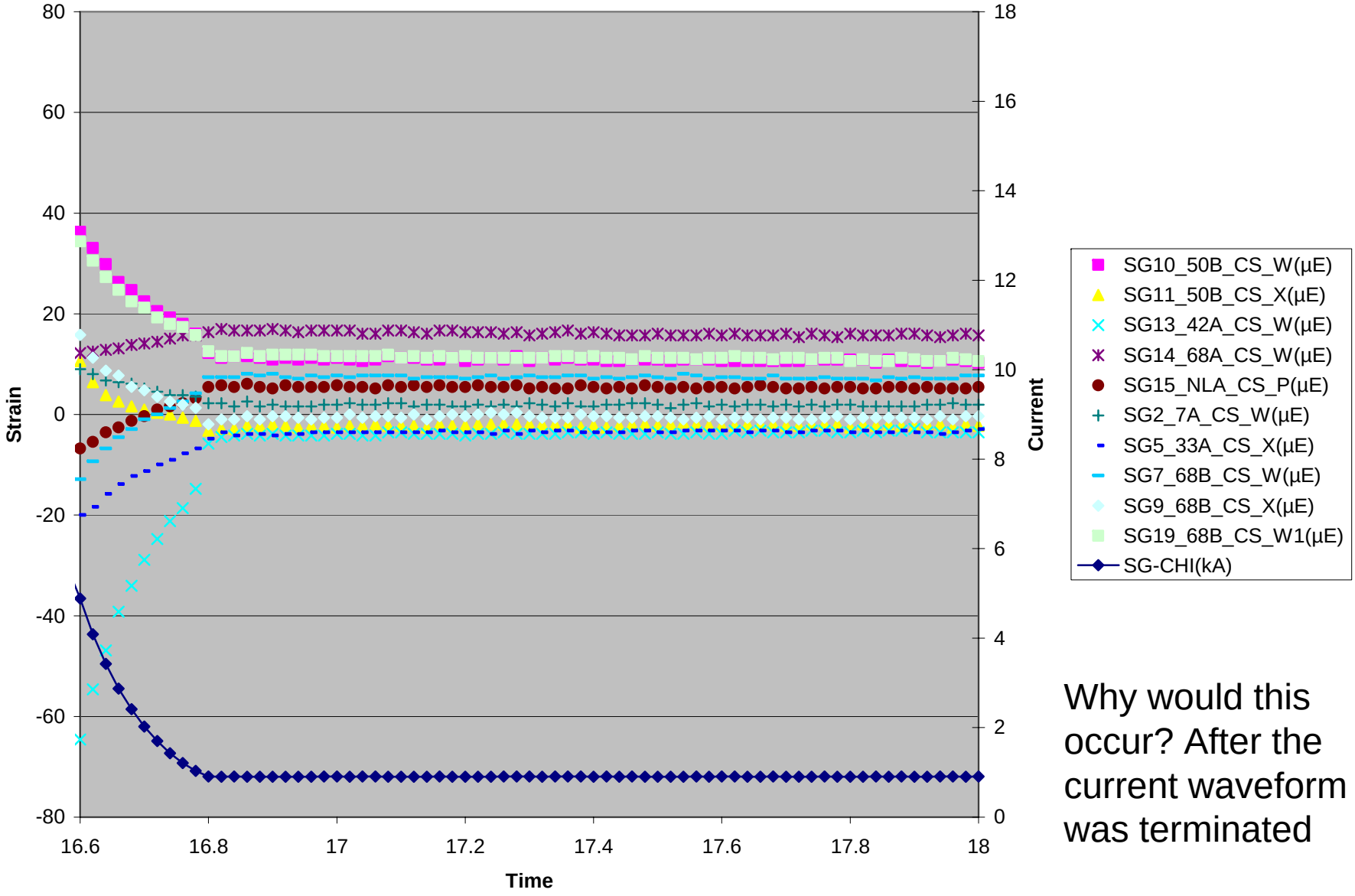

Why would this occur? After the current waveform was terminated

What about the other trips (35 Amp cold) 121412

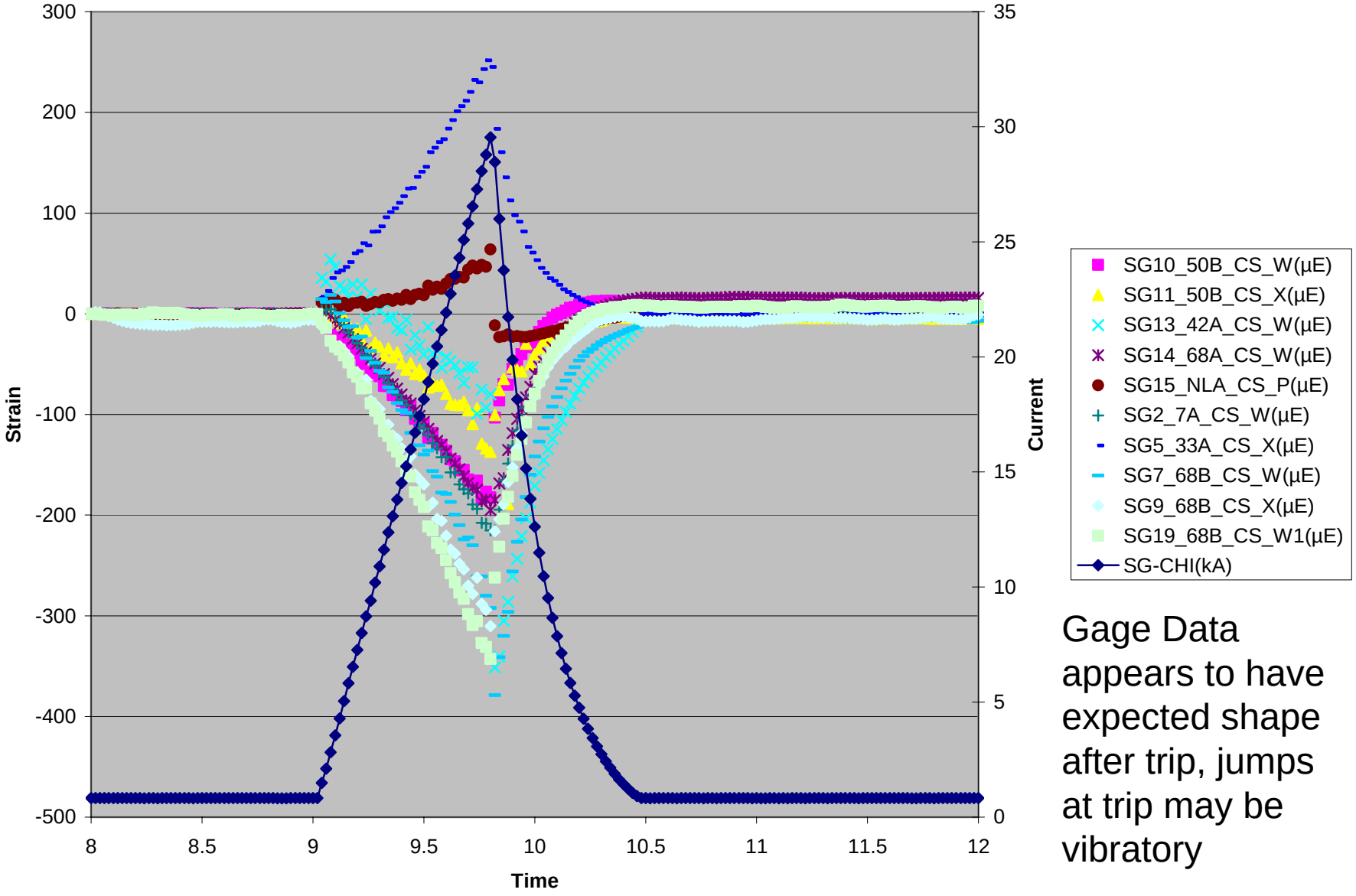

Gage Data appears to have expected shape after trip, jumps at trip may be vibratory

36.5 Kamp Case (121461)

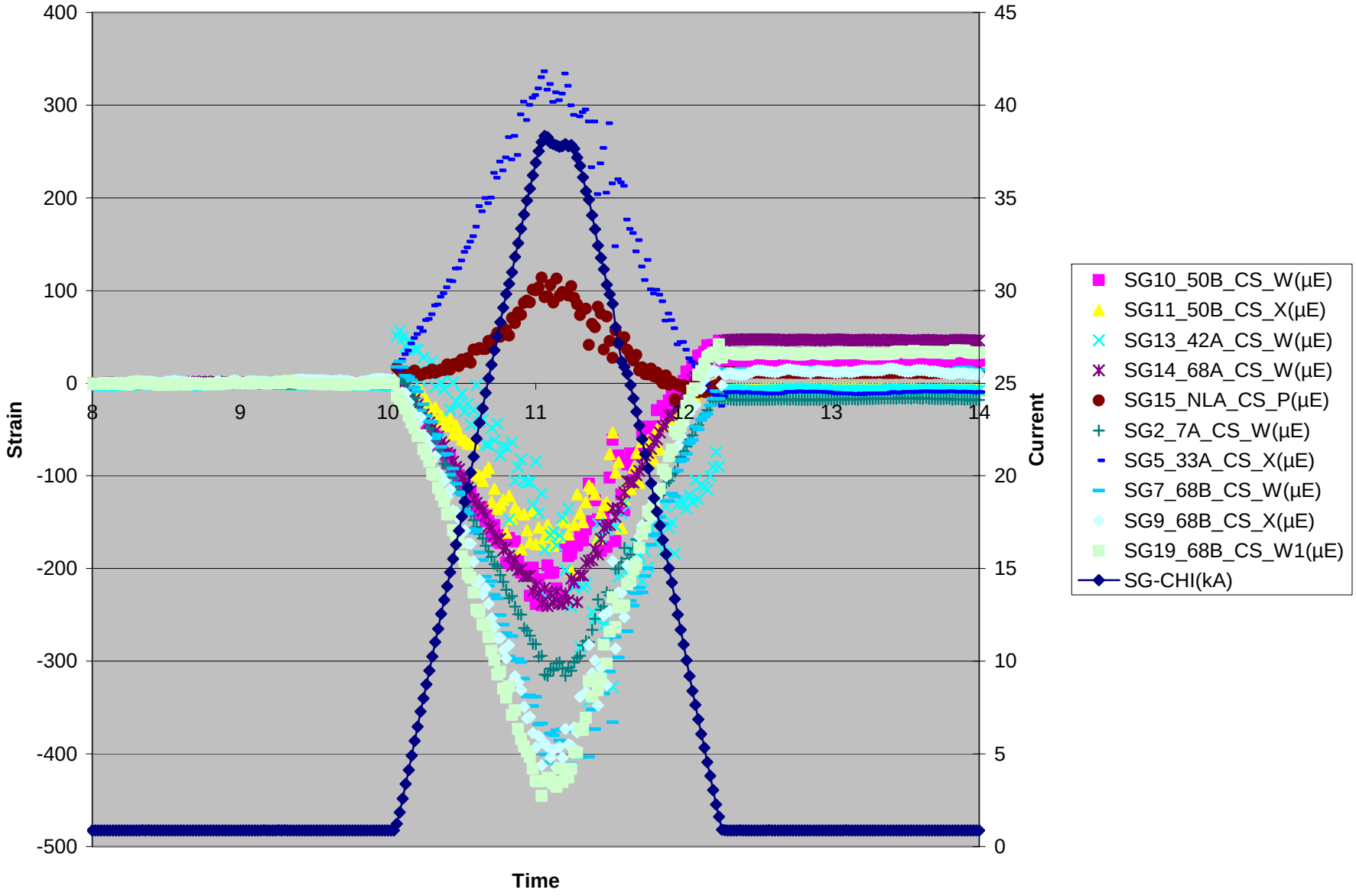

Winding Gage Plots

15 kamp Cold

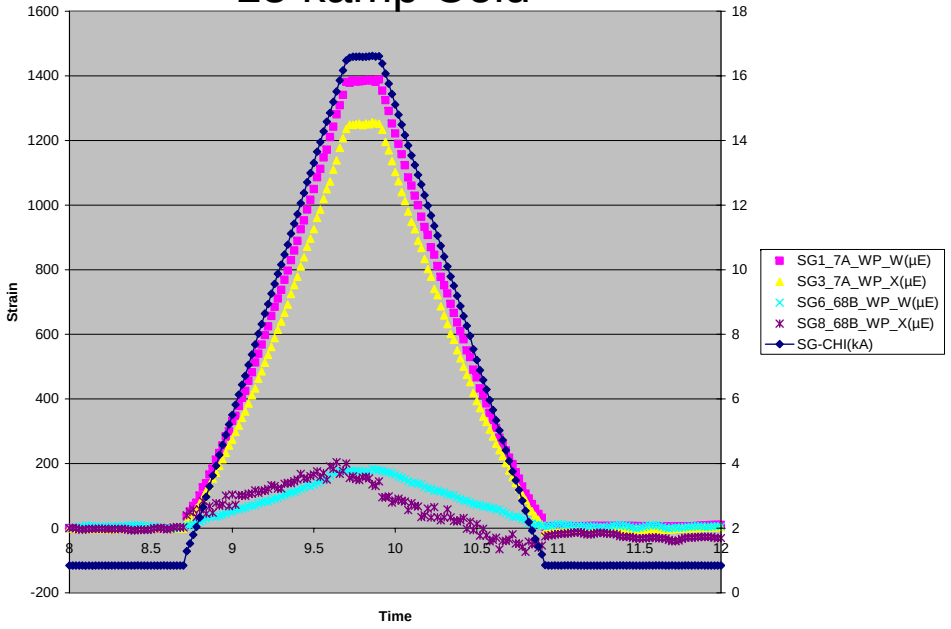

15 kamp Warm

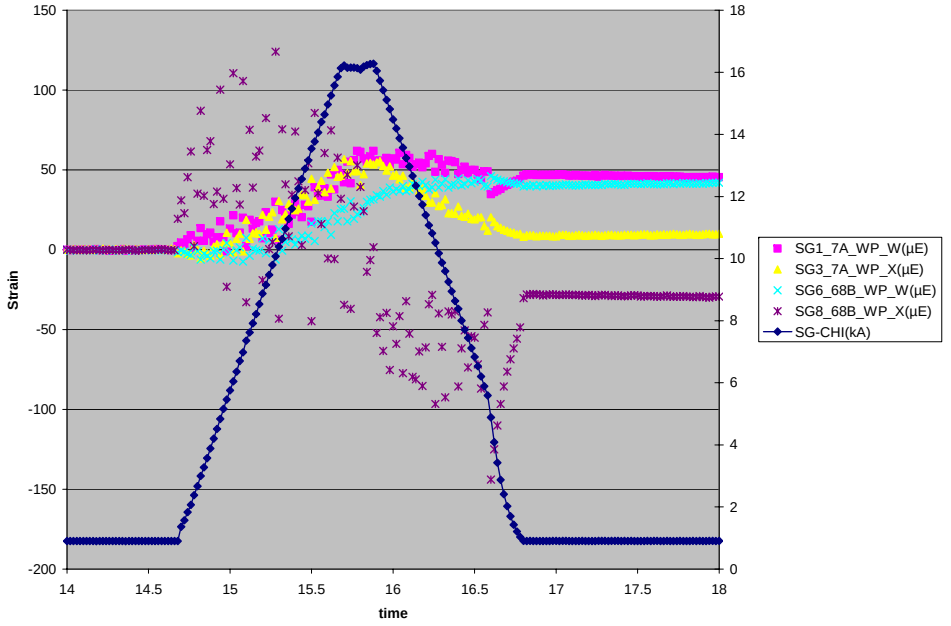

35 kamp Trip

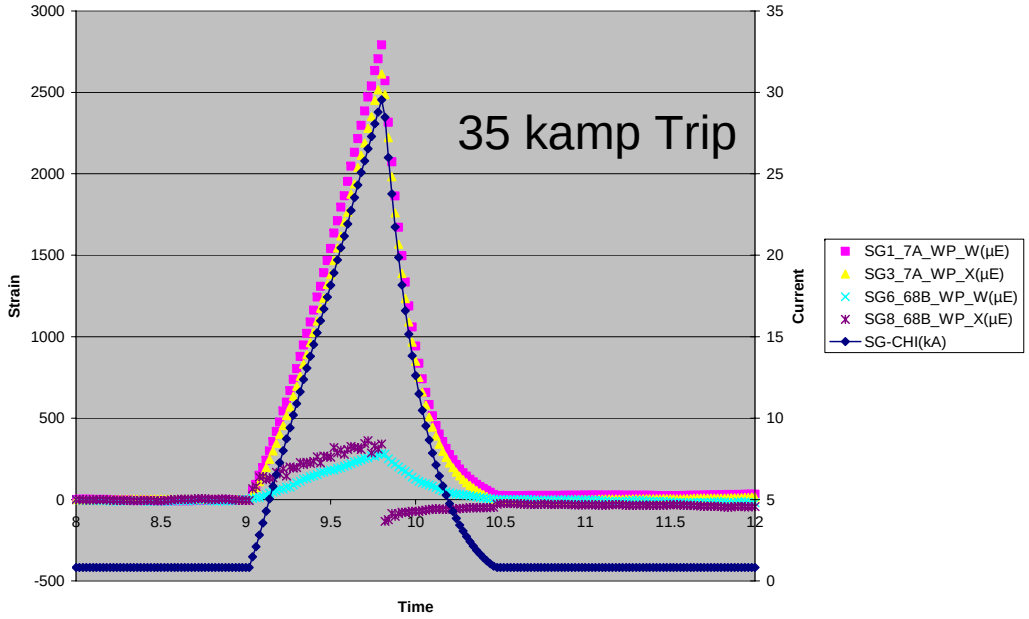

Hole strain comparison for shot 121461

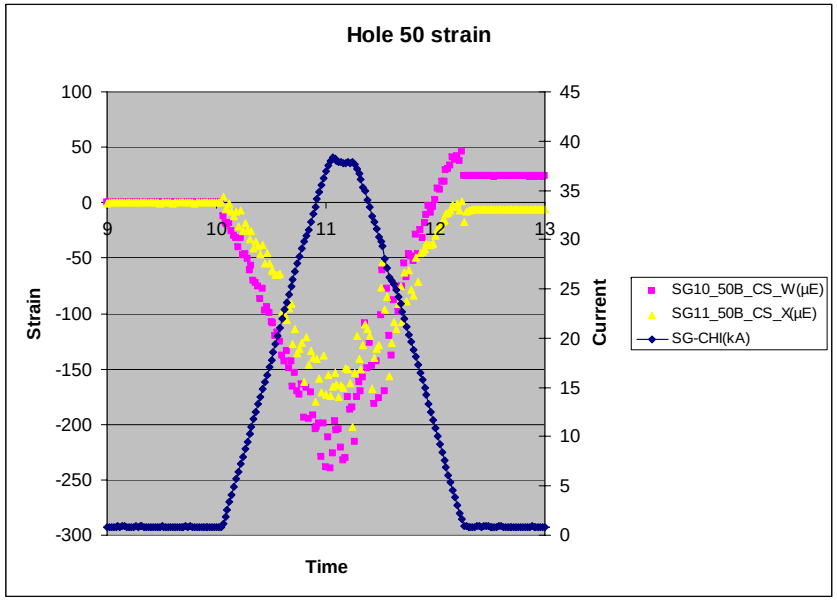

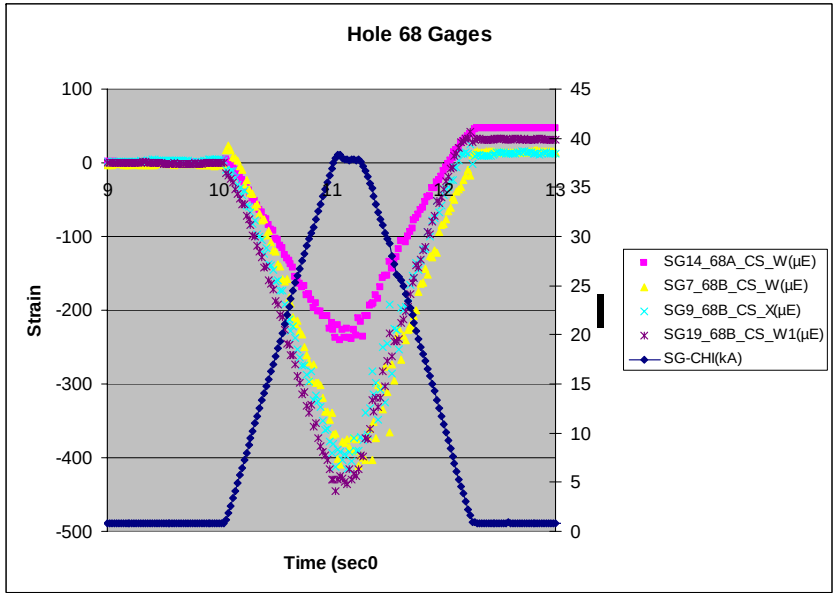

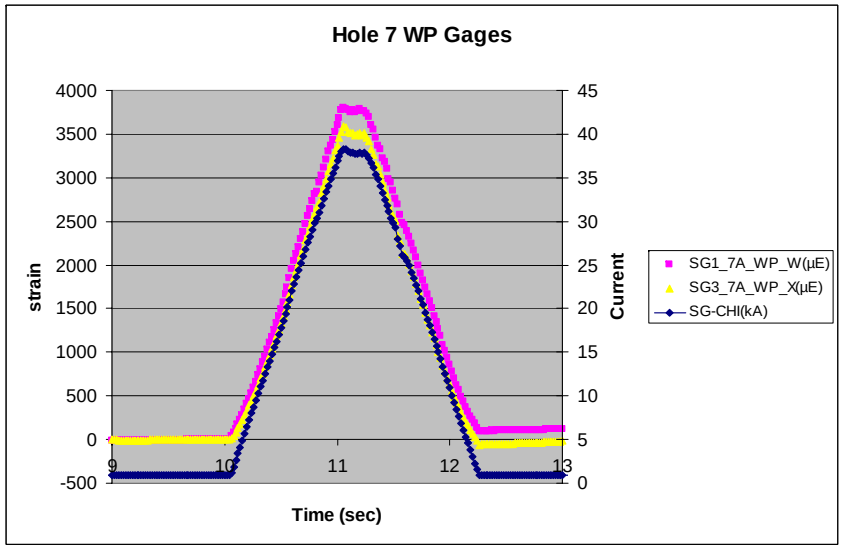

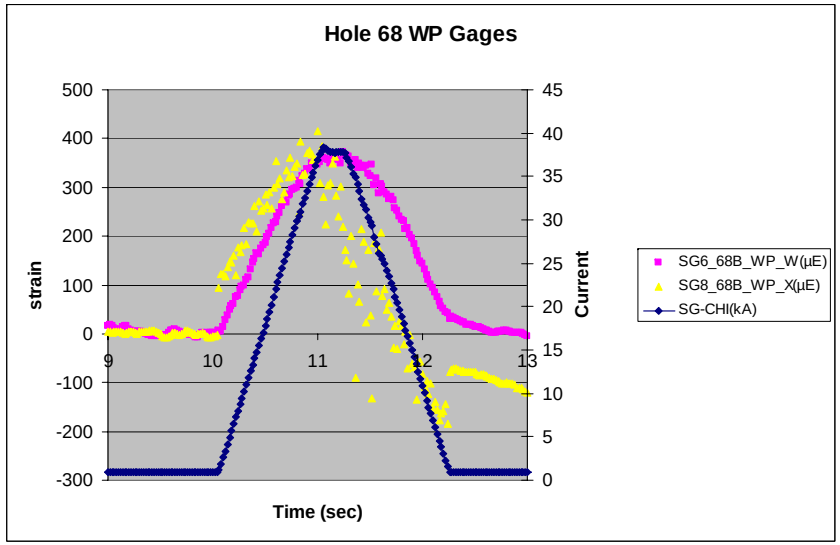

Very Little chance that strain in two directions measured on like holes would be the same

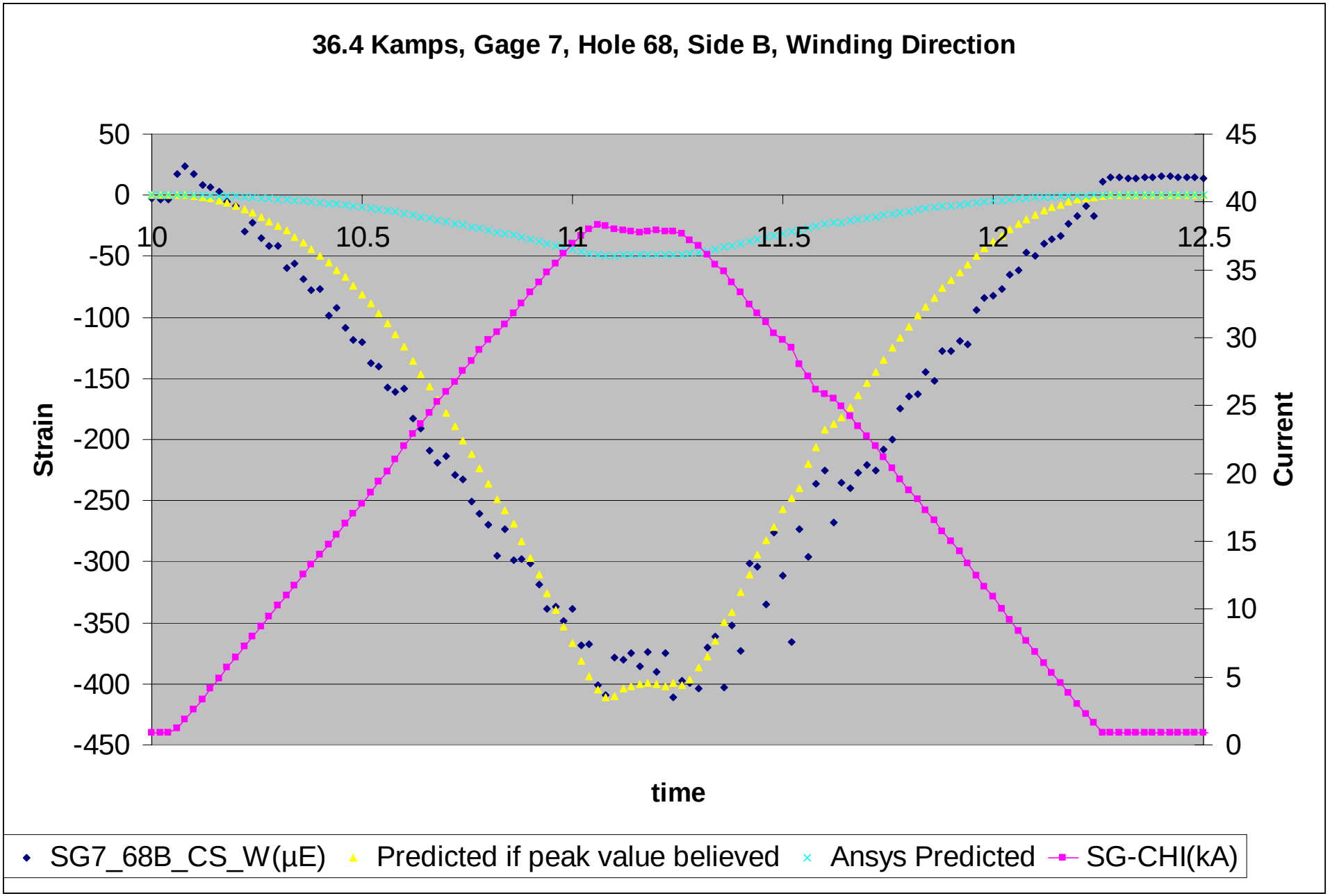
36.4 Kamps, Gage 7, Hole 68, Side B, Winding Direction
50
0
-50
-100
-150
-200
-250
-300
-350
-400
-450
Strain
10
10.5
11
11.5
12
12.5
time
45
40
35
30
25
20
15
10
5
0
Current
SG7_68B_CS_W(µE)
Predicted if peak value believed
Ansys Predicted
SG-CHI(kA)

Points

- Data does not match ANSYS in direction or magnitude except gage 15
- Strain readings in different directions at the same hole number give roughly the same delta strain.
- Turning the current off (Trip) seems to create a different strain profile for both cryogenic and room.
- Room data is all over the place and loosely follows a voltage profile for most gages.
- Cryogenic data is highly linear while the current is being controlled (voltage applied).
- Gage 15 away from the coils near the leads looks somewhat plausible even at room temperature. (Were its wires wrapped around the windings?)

7 PHOTOGRAPHS OF THE TEST SETUP

Figure 7-1 Cryostat carriage in fabrication

Figure 7-2 Cross-section of 4-conductor current feed with fiberglass angle supports

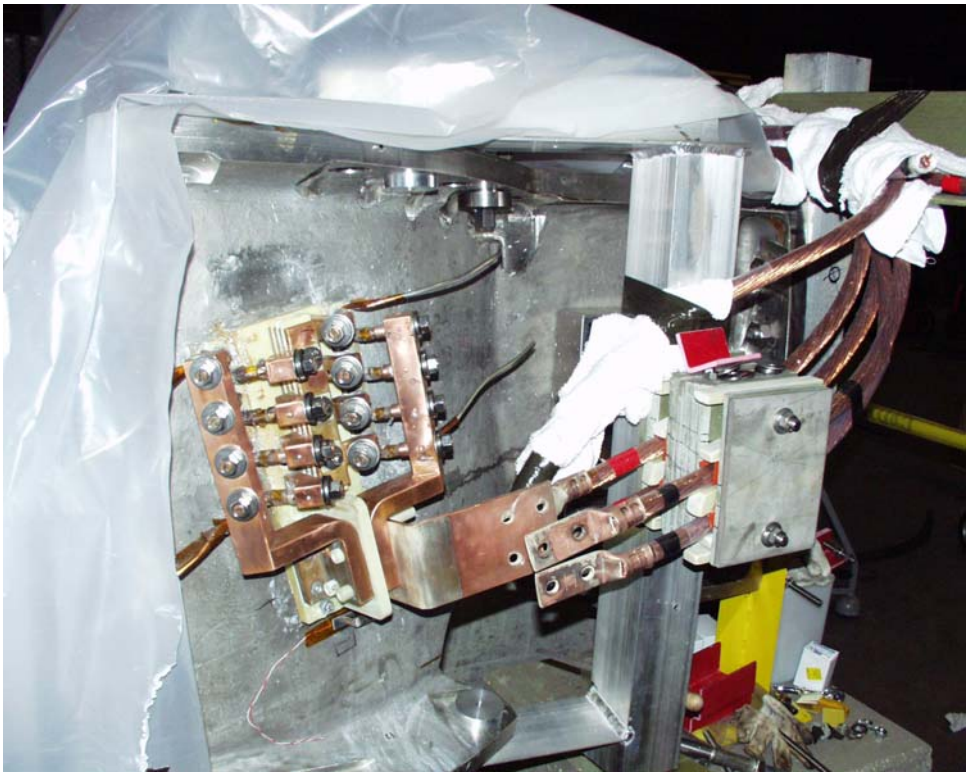

Figure 7-3 Connection of current feed to C1 coil

Figure 7-4 Crimped lugs on current feeds

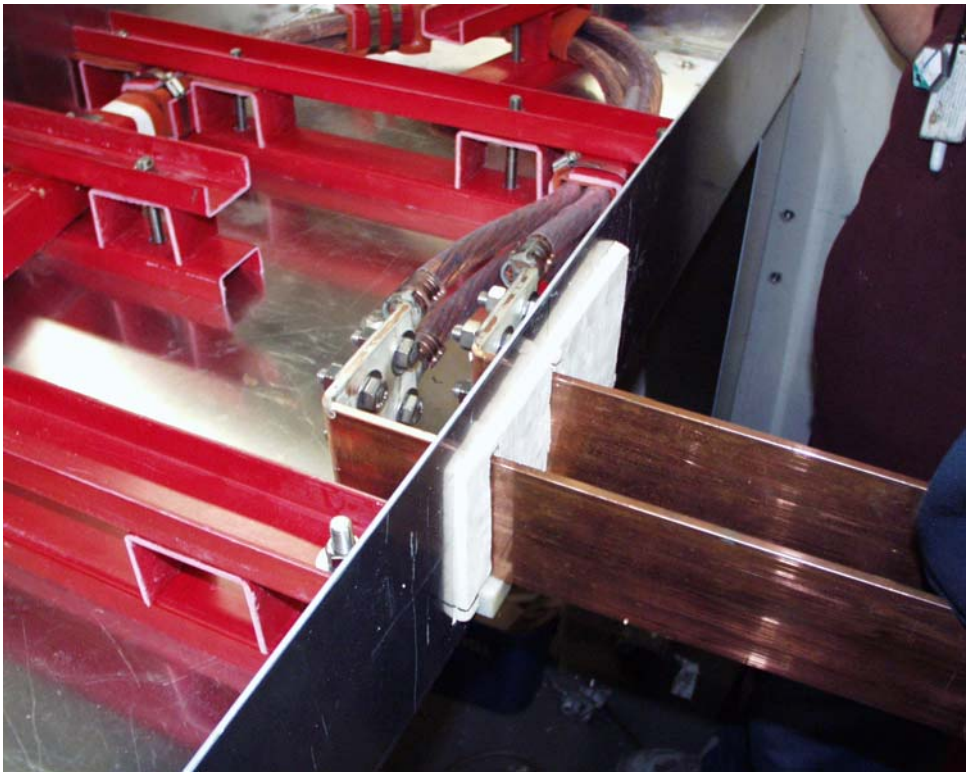

Figure 7-5 Bus connection to 4-conductor current feed inside thermal transition box

Figure 7-6 Connection of cryostat to facility exhaust

Figure 7-7 Cryostat inside Coil Test Facility

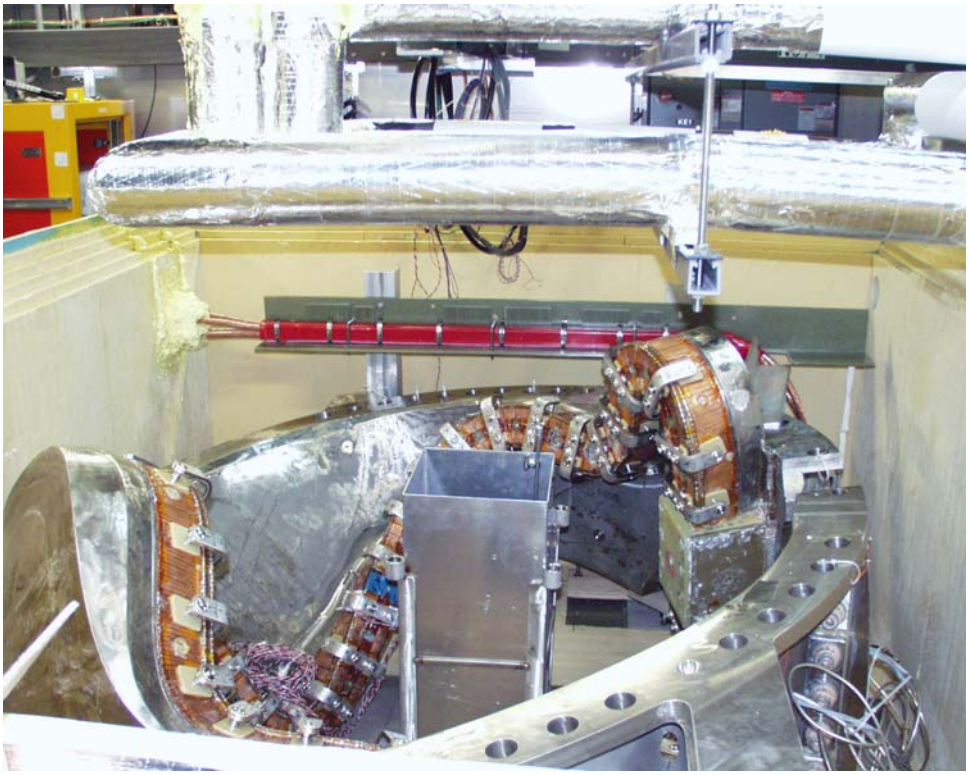

Figure 7-8 C1 coil inside cryostat

Figure 7-9 Restraints on C1 supports

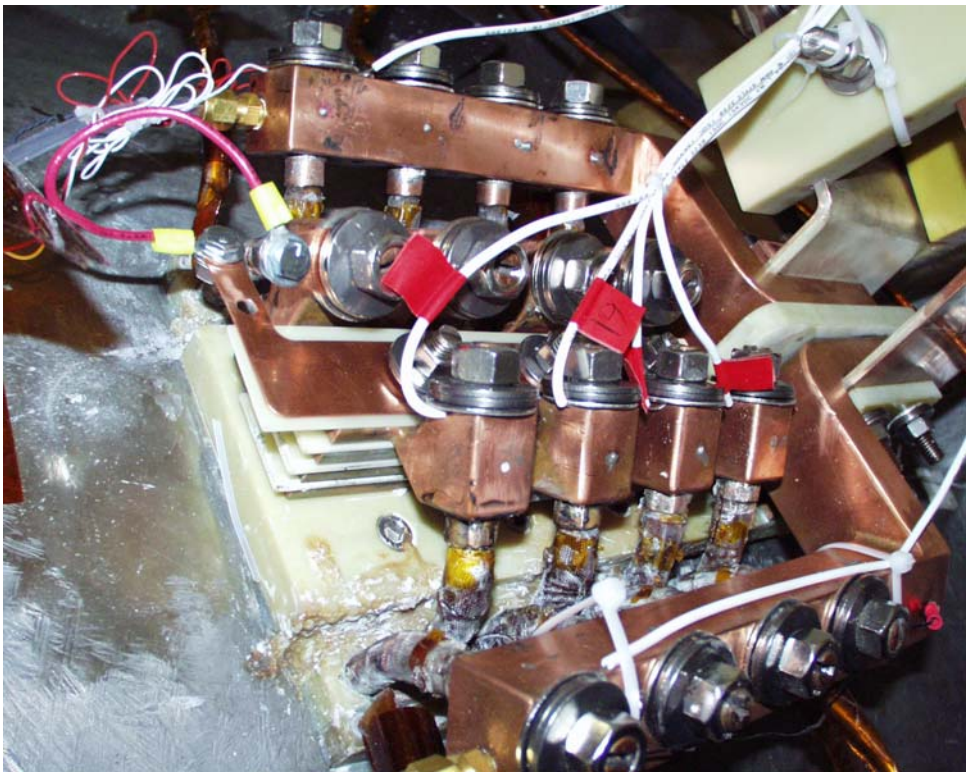

Figure 7-10 Instrumentation of jumper assembly

Figure 7-11 Strain gages at Clamp 68 - Side B

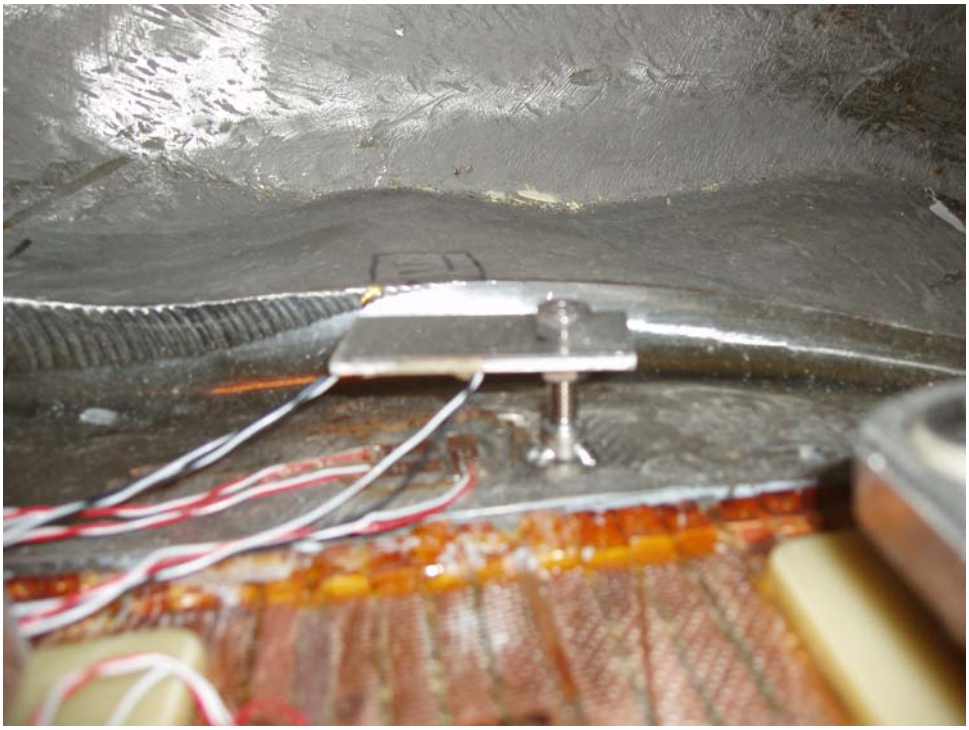

Figure 7-12 Casting strain gages at Clamp 68 - Side B

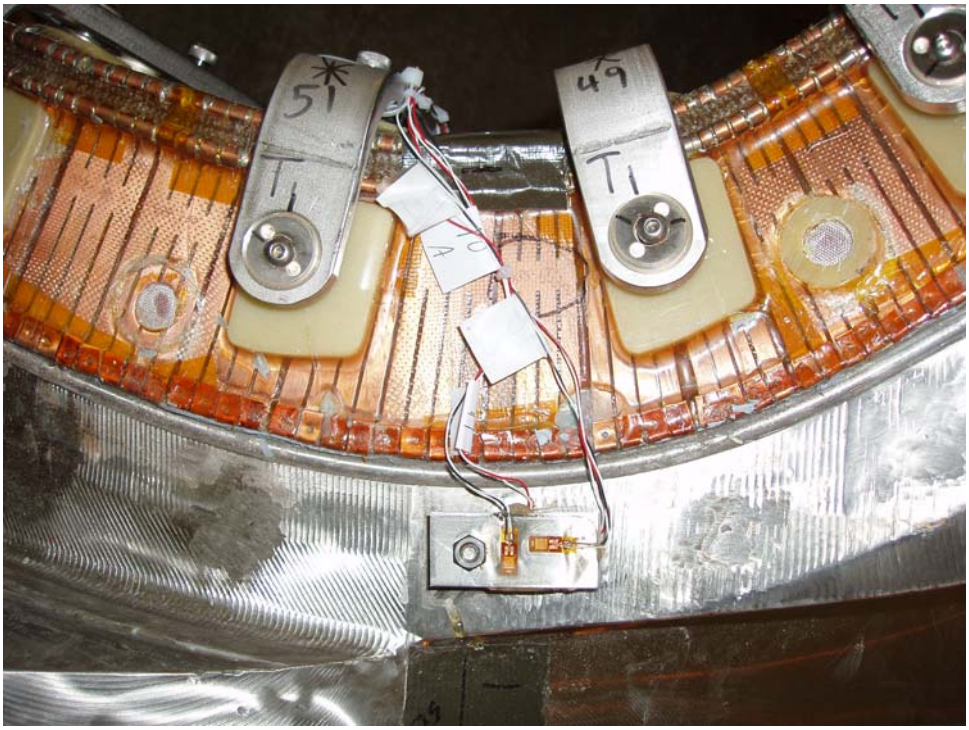

Figure 7-13 Strain gages at Clamp 50 - Side B

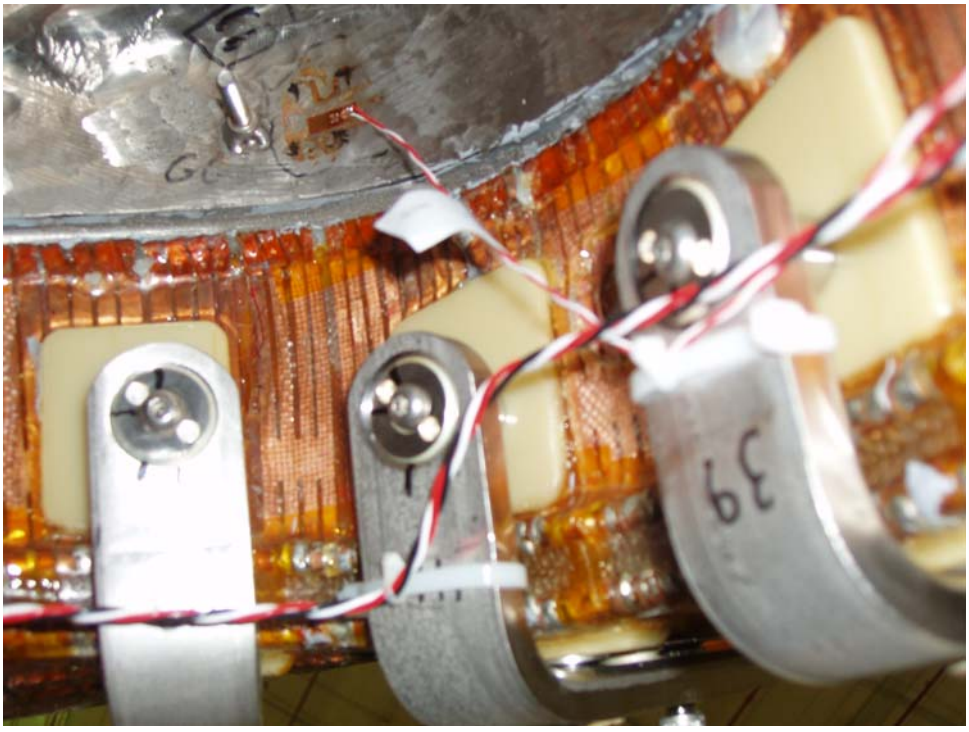

Figure 7-14 Strain gage at Clamp 42 - Side A

Figure 7-15 Strain gage (SG15) near lead block

Figure 7-16 Winding pack strain gage (dummy) at Clamp 7 - Side B

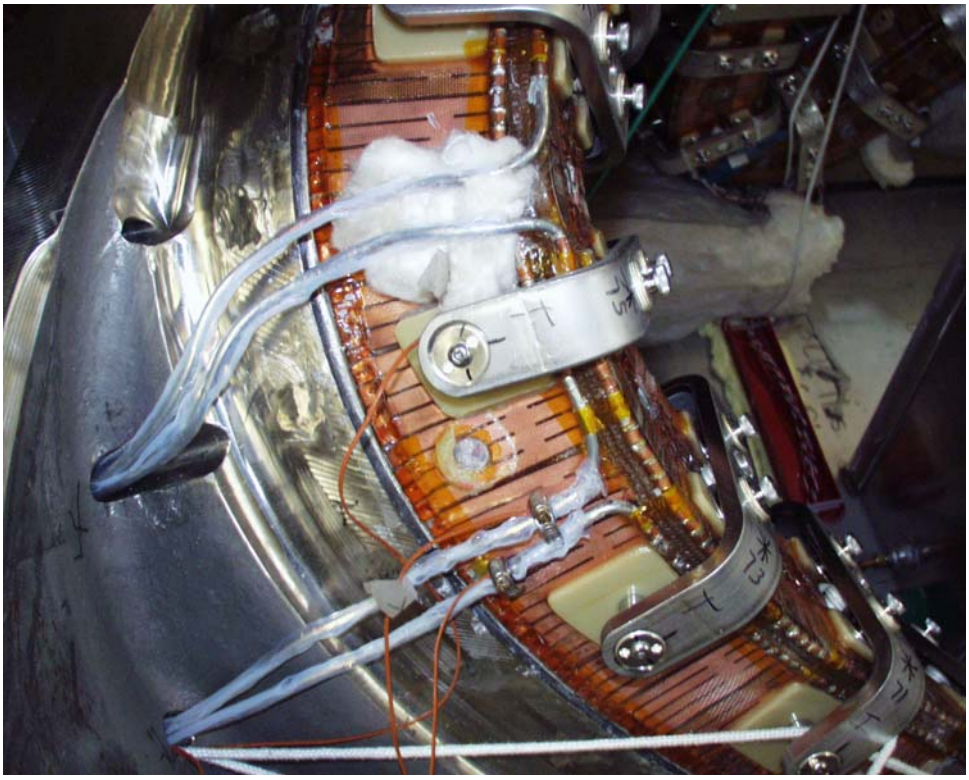

Figure 7-17 Winding pack thermocouple (TC17) under glass wool